ISSN: 0974-5823 Vol. 7 (Special Issue 5, April-May 2022)

International Journal of Mechanical Engineering

DEVELOPMENT OF A MODULAR L-BAND PROFILER FOR ATMOSPHERIC BOUNDARY LAYER AND PRECIPITATION STUDIES

[1]Dr.P. Srinivasa Rao , [2] Dr. Medikonda. Christhu. Raju, [3]B. Alekhya, [4]Kaaparapu. Satish Babu

[1]CVR College of Engineering, Hyderabad-501510, India.

[2,3] VNR Vignana Jyothi Institute of Engineering and Technology,hyderabd,500090, India

[4]Geethanji college of Engineerig and Technology, hyderabd,501301, India

Abstract:

The proposed paper aims to develop a modular L-band CW radar for studying precipitation and processes in the Atmospheric Boundary Layer (ABL). The system can be operated either in vertical or off-vertical modes, enabling us to derive winds. The range resolved scattering coefficient C_n^2 will be obtained from the signals received. The system makes use of 1024-bit linear maximal length code or complementary code pairs modulating the carrier of 1.4 GHz with a baud time of 250 ns or 100 ns to get a range resolution of 37.5 m or 15 meters. The linear maximal length code is repeated after 1024 clock cycles and the Radar operates almost in CW mode. In the case of complementary code velocity vectors. The radar transmitter and receiver are co-located. The radar makes use of independent antennas for transmitter and receiver with enough separation for isolation. Radar probes the ABL and the data is obtained from layers that are 84 m above ground level. Pairs, the PRF is up to 4000. Doppler shifts will be obtained by the FFT technique as well as by the maximum entropy method for computing radar makes use of independent antennas for transmitter and receiver with enough separation for isolation. Radar probes the ABL and the data is obtained from layers that are 84 m above ground level. Pairs, the PRF is up to 4000. Doppler shifts will be obtained by the FFT technique as well as by the maximum entropy method for computing

Keywords: ABL Layer, FFT technique, Doppler Shift and Lidar

1.0 Introduction:

Lower troposphere region of the Earth's atmosphere including Atmospheric Boundary Layer (ABL) is not static single temperature environment. It is a swirling mass of gases at different pressures and temperatures. In addition to this there is also varying amounts of water vapour in ABL and with varying refractive index. Normally temperature in troposphere decreases with altitude but under certain conditions inversion in temperature can occur with corresponding change in Radio refractive index. The study of water vapour and precipitation

will be useful for understanding the cloud physics which in turn helps in understanding weather. Construction of Pulsed Doppler Digital Receiver is explained in [1].effect of Doppler extraction from SODAR using complex covariance technique is explained in [2]. Refraction and Partial Reflection Radar for the measurement of Mesospheric in free space is studied in [3].

High Frequency Backscatter Radar at the magnetic equator is compared with existing methods [4]. Studies on tropospheric aerosol layers at a tropical coastal station was referred in [5]. Light detection and ranging (Lidar) observations of cirrus clouds at low latitude tropical station is referred [[6]. High-Resolution Imaging Laser Altimeter for Interplanetary Missions are referred in [7]. How Temperature varied or depends on stratospheric aerosol extinction observed at a low latitude station [8]. Cirrus clouds observed near the low latitude tropical tropopause using the ground-based Lidar technique is in [9].

The minimum altitude from which we get the signals depends on parallax error and far-field distance. Parallax is due to the separation of the transmitting antenna and the receiving antenna and beam overlap even though they are co-located. Beam overlap factor $C_P(R) = e^{-2\ln 2\frac{d^2}{\delta\theta^2 R^2}}$ Where R is the range $\delta\theta$ is beam width and d is the separation between the two antennae. Far-field distance $= \frac{2D^2}{\lambda}$ Where D is the diameter of the dish antenna and λ is the wavelength for the dish size of 3 meters and for carrier frequency of 1.4 GHz, the far field distance is 84 m. These two factors have to be accounted for in the received signals from the near field. Explained about microwave refractometry [21], studied about radiosondes and rocketsondes [22], glance look about GPS and Lidar measurements [23], [24],and the refractivity from clutter technique studied [25]–[28]. Some meteorological models such as the Coupled Ocean/Atmospheric Mesoscale Prediction System (COAMPS) [29] and models based on Monin–Obukhov similarity theory (MOST) [10] such as the Navy Atmospheric Vertical Surface Layer Model (NAVSLaM) [11], [12].

2.0 Properties of Atmospheric Layer: Refractive index always present in free space and it is variable and it is given by

$$M = N + h/a \times 106 \approx N + 0.157h$$

Where earth is in circular in shape and has radius a and h is the refractive index value from earth boundary.

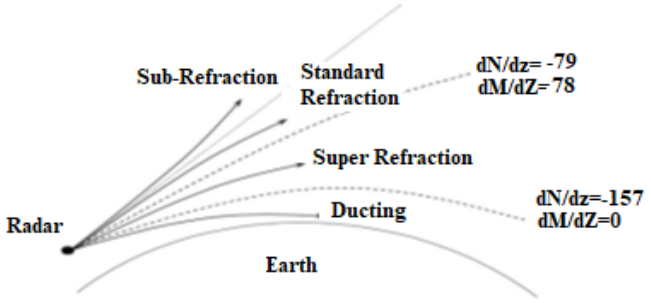

Fig 1. Shows the standard refractive index variations. When rays / signals are transmitted from the transmitter horizontally. Above figure shows the height of duct from earth, super refraction, standard refraction and sub refraction.

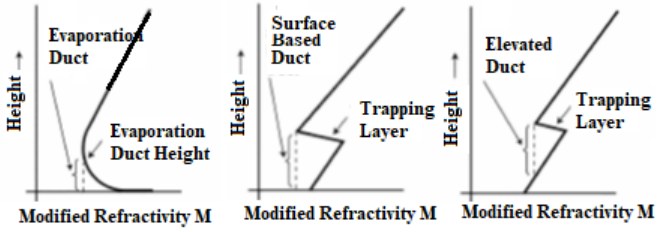

Fig. 2. In the figure variation of the refractive index in free space with some distance from earth is shown as a duct. Ducting is again classified into three types as shown.

3.0 Proposed Work

Our proposed radar system will be located in a semi-urban area of Hyderabad which experiences a very dry climate during summer and winds blowing and carrying a lot of dust and pollutants are not uncommon. Also, the place experiences high humidity conditions before and during monsoon and receives rainfall during both SW and NE monsoons.

The proposed transmitter and receiver systems are transportable which provides flexibility in positioning them. This enables us to study turbulence in the medium at any given location. The receiver system receives signals from clear air atmosphere (which are very weak) precipitation and biota (like insects and birds) which give strong signals. To cater to the wide dynamic range of received signals more than 80 dB dynamic range will be provided in the receiver system. The receiver system makes use of a properly matched filter for getting the maximum signal-to-noise ratio. The medium (ABL) covered is from almost ground level to 3 km depending on the separation of the transmitter and the receiver antennas.

Precipitation can be studied during these monsoon periods. As the system can be operated continuously it is possible to study diurnal and seasonal variations. Hyderabad is at an altitude of 500 m above the mean sea level and at a distance of 300 km from both sea coasts. Also, it is one of the most polluted cities in the country.

- The radar works at a carrier frequency of 1.4 GHz by using linear maximal length pseudo random code or complementary code pairs with baud time of 250 ns or 100 ns and providing a range resolution of 37.5 m or 15 m.
- The radar works at a PRF of 4000 providing adequate number of samples for averaging for SNR improvement in a given time.
- The peak power of the transmitter is 20 Watts.

The sensitivity of the receiver is -100dBm

1. For 0 dBz the minimum expected signal level is -34 dBm and for -20dBz minimum expected signal level is -54 dBm
2. The system specifications are adequate for studying precipitation and clear air atmosphere with C_n^2 above 10^{-14}

3.1 Radar (Transmitter) Specifications

- Radar operating frequency: 1.4 GHz
- Radar Type: Pulsed capable of in working in continuous mode,
- Type of transmitter pulse: Phase coded (complementary codes or linear maximal length codes)
- PRF: 1000 to 4000 [25% duty ratio to 100% duty ratio]
- Peak Power: 20 Watts
- Average power: 5 W to 20 W depending on the duty ratio [25% to 100%]
- The Radar operates in Bistatic mode using independent Antennas for transmission and reception. Sufficient isolation is provided between the two antennas to avoid leakages. Reception is possible while the transmission is going on. The target will be hit by the transmitted pulse and the received echo signal from the target will be on a continuous basis. The maximum length of the pseudorandom code is 1024 bits. There will not be any problem of unambiguous range. This radar works like FMCW radar with the only difference of instead of using a Linear FM signal for transmission linear max length code modulated RF is used. The duty ratio can be high like in Linear FM Radar systems.
- Transmitter type: solid-state
- Transmitting antenna: 3m diameter parabolic dish with a gain of 848.25 or 29.2 dB
- Antenna Beam width: 5.7^{O}[$1/10^{th}$ radian]
- Baud Time of code: 250ns or 100 ns.
- Range resolution: 37.5m or 15 m. [Range accuracy can be improved to 6 m by using sliding correlators if SNR permits]
- Maximum code length: 1024 bits

3.2 Radar Receiver Specifications:

- Operating frequency: 1.4 GHz
- Receiver Type: Digital Receiver, phase-coherent, digitizing at IF and Digital Down conversion to video signals
- Receiver Sensitivity: -100 dBm
- Receiver Dynamic range: 90dB
- Receiver Antenna: 3m diameter parabolic dish with a gain of 848 or 29.2 dB

- Receiver Beam width: 5.7º[1/10th radian]
- Receiver Bandwidth (2 way) : 8 MHz / 20 MHz
- I & Q imbalance: Less than 0.1% in amplitude and less than 0.25^0 in phase angle.

3.3 Radar Controller and Processor Specifications:

- Radar Controller Type: PC-based.
- Radar Signal Processing: Demodulation of the received signals to baseband I & Q information using FPGA-based digital correlators followed by coherent integrators.
- Extracting the Doppler information from coherently integrated I & Q information's.
- Signal to Noise Ratio enhancement after getting power spectra from I& Q information.
- Doppler information extraction either by FFT technique if sufficient data is available otherwise by Maximum Entropy Method. Velocity vectors will be computed from the spectral data.
- Total Processing: ' ON ' line

4.0 Different Modes of Operations of the RADAR: 4.1. Colocation Mode of Transmitter and Receiver Antennae: a). Vertical Beam: Sounding the boundary layer in vertical mode : Problem in this mode: Non overlapped Transmitted beam and receiver field of view in the near field (up to 84m for 3m dish antenna and 1.4GHz frequency). In the near field the transmitted wave has to be considered as a planar wave rather than a wave getting emitted from a point source.

- In this mode only velocity vector in the zenith direction only will be obtained.
- The following plot shows the transmitter beam and receiver beam with respect to horizontal range and altitude coverage.

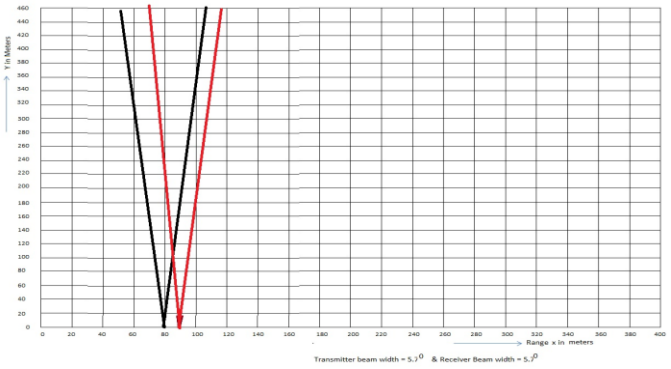

Fig 3. Vertical Beam transmission in Colocation Mode of Transmitter and Receiver Antennae

b) Slant Beam:

- Sounding the boundary layer using Slant Beam.
- In this mode, the radar transmits in a slant direction, and the receiving antenna looks at the same illuminated volume of the transmitted beam.
- The separation between the two antennas has to be properly adjusted correction factors have to be applied for parallax error and near field up to an altitude of 84 m.
- The following plot shows the transmitter beam and receiver beam with respect to horizontal range and altitude coverage.

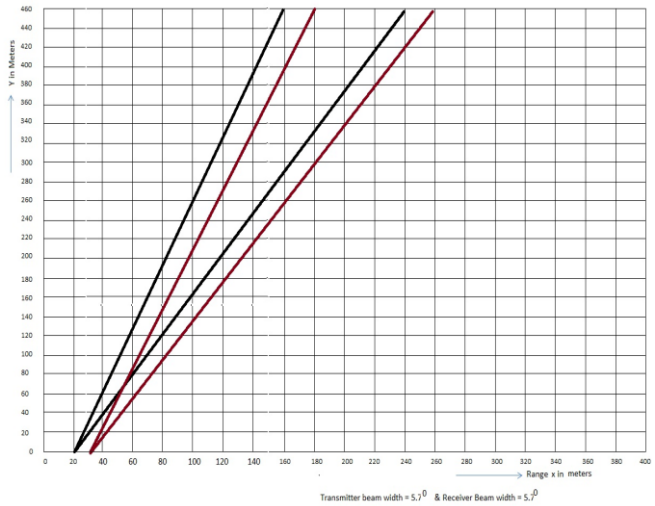

Fig 4. Slant Beam transmission in Colocation Mode of Transmitter and Receiver Antennae

4.2. Bistatic mode of operation

- A particular volume of the boundary layer can be studied as shown in the diagram.
- Phase coherence has to be maintained between transmitter and receiver.
- The transmitter and receiver are separated by distance of up to 1km.

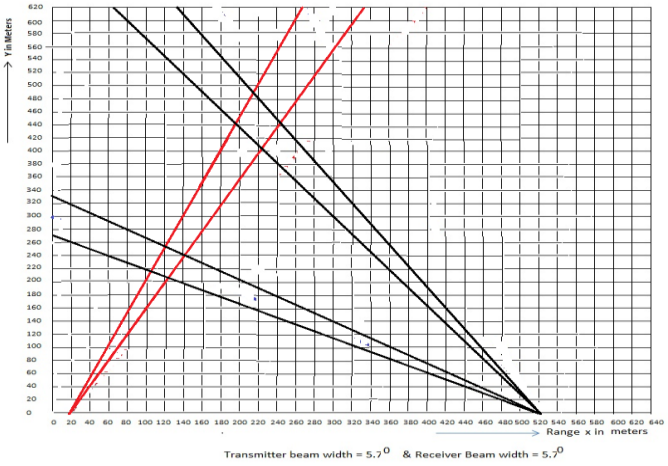

Fig 5. The graph shows the Bistatic Mode of operation

- The RF wave has to be carried to the receiver through cables which is expensive or the RF wave has to be derived from the receiver signals by a carrier recovery circuit by removing the modulation effect. Otherwise initially carrier has to be transmitted without any modulation for synchronization.
- The following plot shows the transmitter beam and receiver beam with respect to horizontal range and altitude coverage for two values of slant angle of receiver beam.

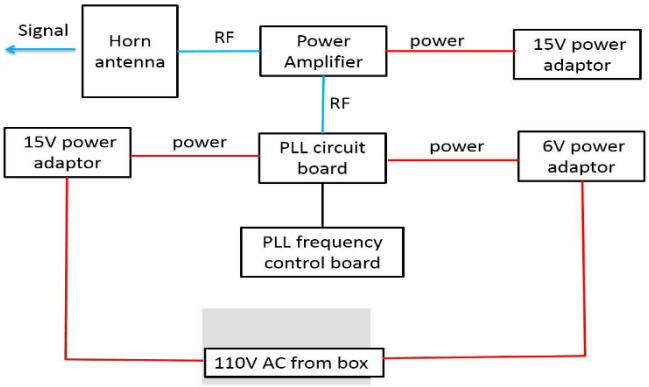

Fig. 6. The figure shows the phase-locked loop which is tuning the frequency and is suitable for PLL frequency board with continuous-wave transmitter with higher gain.

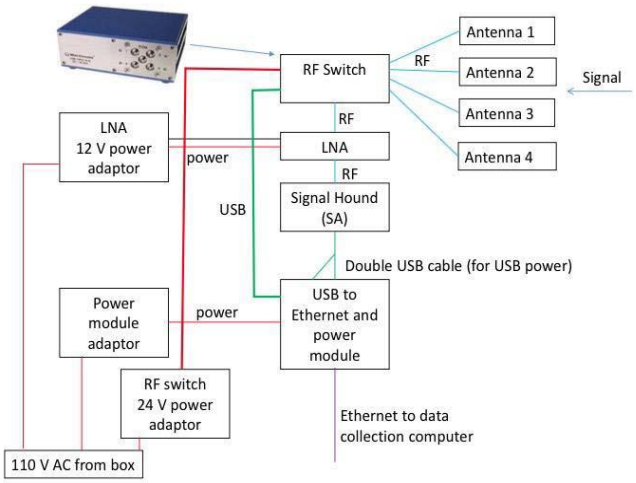

Fig 7. High-gain CW Receiver

5.0 TYPES OF ATMOSPHERIC CONDITIONS TO DEAL WITH BY THE RADAR.

a). Clear Air Conditions:

Power aperture product is the main design parameter to be computed using system parameters and atmospheric reflectivity. The block diagram shown below is referred to in the following signal to Noise Ratio computations for both clear Air condition and cloudy condition.

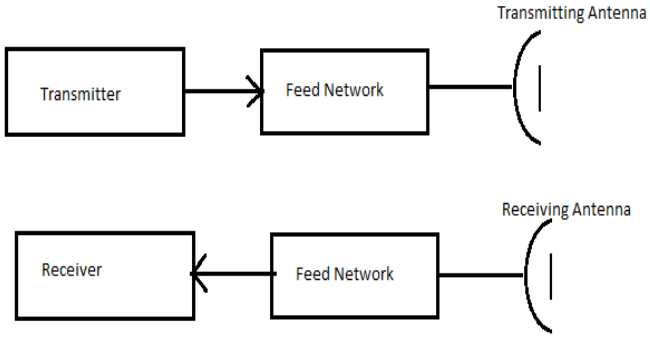

Fig 8. General Block diagram of RADAR

The effective transmitter power gets reduced by a factor L_T called Loss Factor. In the receiver path, the feed network with attenuation L_R precedes the receiver front end. As a result, the effective noise figure of the receiver (Noise Factor) gets enhanced by $L_R F_R$ where F_R is the Noise figure of the receiver system. Therefore the effective Noise Temperature of the receive path will be ($L_R F_R$ -1) to the received signal power

$$P_S = \frac{P_t A_e}{L\, 2 Log_e 2 4\pi R^2}\left(\frac{C\tau}{2}\right)\left[0.38 C_n^{\,2}\, \lambda^{\frac{-1}{3}}\right]$$

$$P_N = K\left[T_c + F_R (L_R - 1) T_o\right] B$$

For 250 ns baud time the following computations are made. For 100 ns baud time, the noise floor goes up by a factor of 2.5. Received signal power comes down by factor of 2.5. Net SNR loss factor is 2.5 * 2.5 = 6.25 (8dB). Where P_t = transmitted power, A_e = Effective area of the antenna, τ = pulse width, $C_n^{\,2}$ = Reflectivity factor of the atmosphere, L_R = Receiver Noise Figure, T_c = Cosmic temperature for the selected frequency of 1.4GHz (15^0 K), λ = wavelength of 1.4 GHz = 0.2143 m, F_R = Noise figure of Receiver = 3.0dB (typical Value) and R= Range (Maximum value 3000 meters).

The ratio $\frac{P_S}{P_N}$ gives the SNR for a single pulse. Generally the single pulse SNR is not sufficient to derive the atmospheric parameters. Large number of radar pulses is transmitted to obtain echoes from different layers of the atmospheric boundary layer (ABL).

Parameter Value	SNR (dB)	R(m)	L_R	τ	$C_n^{\,2}$	T_c (^{0}K)	FR (dB)	Optimum B.W(MHz)
	-50	300	1	25 ns /10 ns	10^{-13} to 10^{-15}	15	3.0	4.8 / 12

Both ON line and OFF line processing techniques are used to improve the SNR. A typical SNR improvement factor of 50 dB is required for $C_n^{\,2}$ of 10^{-13}. Received Signal Power for $C_n^{\,2}$ = **10^{-15},** $P_S = \frac{P_t A_e}{L\, 2 Log_e 2 4\pi R^2}\left(\frac{C\tau}{2}\right)\left[0.38 C_n^{\,2}\, \lambda^{\frac{-1}{3}}\right]$, The following computation is done for 250 ns Baud time. The signal power P_s comes down by a factor of 2.5 for 100 ns Baud time. Let P_t = 20 W, $A_e = \frac{\pi D_a^{\,2}}{4}$, L= Loss factor= 1 (assumed), K= Boltzmann's constant = 1.38 X 10^{-23} J/Hz, T_C = cosmic temperature = 15 ^{0}K (for our chosen frequency of 1.4GHz). Hence for D_a = 3m $c_n^2 = 10^{-15}$, R=3000m the signal power is

$$P_S = \frac{20 \times \frac{\pi 3^2}{4}}{1 \times 2 \times Log_e 2 \times 4\pi (3000^2)}\left(\frac{3\times 10^8 \times 250 \times 10^{-9}}{2}\right)\left[0.38 \times 10^{-15} \times (0.2143)^{\frac{-1}{3}}\right]$$ This requires an enhancement of 63 dB in SNR to make

$$= 2.144\, X 10^{-20}\, Watts$$

Signal equal to Noise. (Noise power =4 X10^{-14} watt). If $c_n^2 = 10^{-13}$ an enhancement of 43dB in SNR is sufficient to make signal power equal to Noise power. Noise Power is calculated as shown below for the above cases. $P_N = K\left[T_c + F_R (L_R - 1) T_o\right] B_R$, F_R = Noise Figure of Receiver = 3dB =2, T_o = Ambient temperature = 300^{o}K, B_R= Receiver band width = 4.8MHz for 250ns baud time, D_a = Diameter of dish antenna, C = 3 × 10^8 m/sec

$P_N = 1.38\times 10^{-23}\left[15 + 2(2-1)300\right] 4.8\times 10^6 \equiv 4.07 x 10^{-14}\, Watts$ P_N : Noise power goes up by a factor of 2.5 for 100 ns Baud time. In our case Power Aperture Product (P_t .A_e) = P_t X $\frac{\pi D^2}{4}$ = 20 X $\frac{\pi x 3^2}{4}$ =141.4 watt $m^{2.}$ Power aperture product P_t. A_e is plotted against range 'R' for different values of Radar Reflectivity C_n^2 of clear Air Atmosphere and SNR ($\frac{P_S}{P_N}$). This factor Pt. A_e goes up by a factor of 6.25 for 100 ns Baud time.

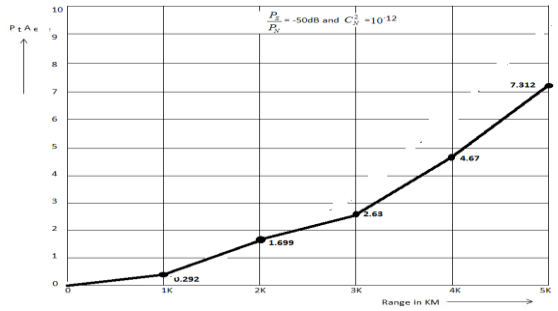

Fig 9. Power Aperture product versus Range for $C_n^2 = 10^{-12}$ and SNR = -50dB

For our radar's 141.4 watt m^2 (P_t. A_e), range covered is beyond 5 km for the above case. For 100 ns Baud time the range covered is also more than 5 km.(P_t. A_e at 5 km = 7.312 * 6.25 = 45.7)

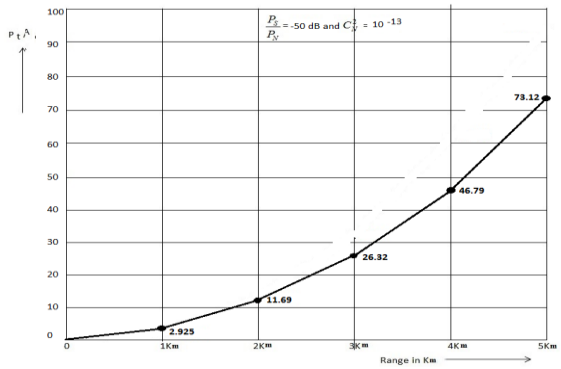

Fig 10. . Power Aperture product versus Range for $C_n^2 = 10^{-13}$ and SNR = -50dB

For our radar's 141.4 watt m^2 (P_t. A_e), range covered is beyond 5 km for the above case. For 100 ns Baud time the range covered is up to 2.5 km.

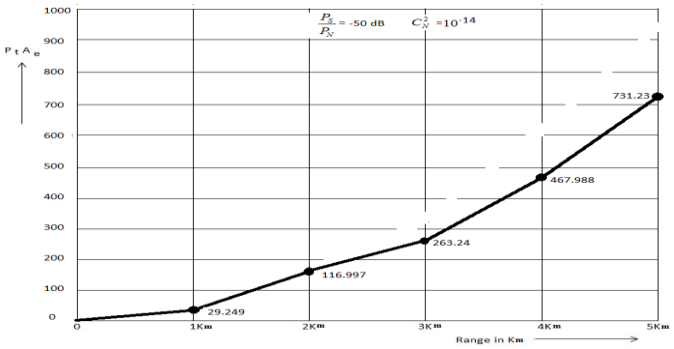

Fig 11. Power Aperture product versus Range for $C_n^2 = 10^{-14}$ and SNR = -50dB for our radar's 141.4 watt m^2 (P_t. A_e), the range covered is up to 2.5 km for the above case. For 100 ns Baud time the range covered is up to 1 km.

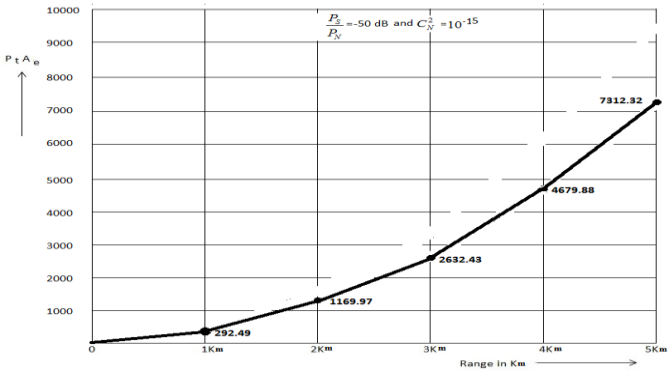

Fig 12. Power Aperture product versus Range for C_n^2= 10^{-15} and SNR = -50dB for our radar's 141.4 watt m^2 (P_t. A_e), range covered is 500 meters. For 100 ns Baud time the range covered is much below 500 meters.

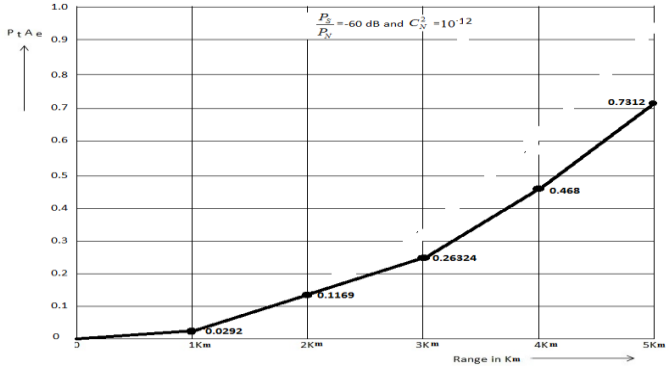

Fig 13. Power Aperture product versus Range for C_n^2= 10^{-12} and SNR = -60dB for our radar's 141.4 watt m^2 (P_t. A_e), range covered is up to more than 5 km for the above case. For 100 ns Baud time also the range covered is more than 5km. (P_t. A_e at 5 km is 0.7312*6.25 =4.57).

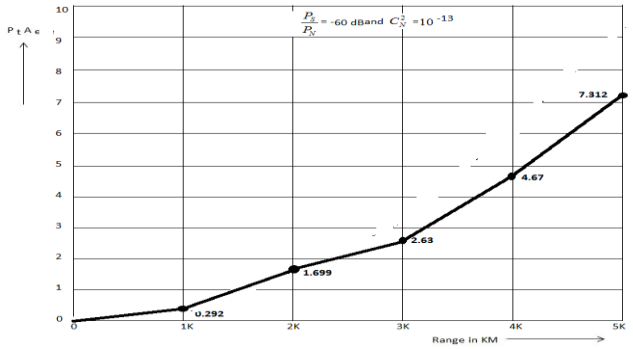

Fig 14. Power Aperture product versus Range for C_n^2= 10^{-13} and SNR = -60dB. For our radar's 141.4 watt m2 (Pt. Ae), range covered is up to more than 5 km for the above case. For 100 ns Baud time also the range covered is more than 5km. (P_t. A_e at 5 km =7.312*6.25 =45.7).

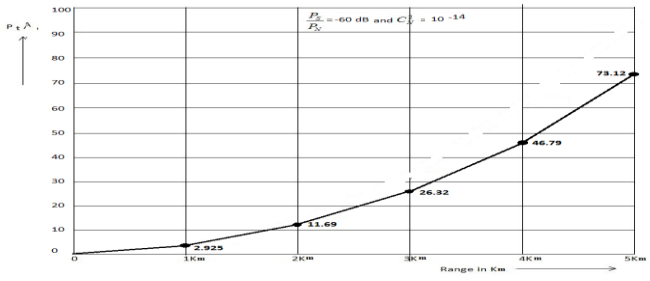

Fig 15. Power Aperture product versus Range for C_n^2= 10^{-14} and SNR = -60dB For our radar's 141.4 watt m2 (Pt. Ae), range covered is up to more than 5 km for the above case. For 100 ns Baud time, the range covered is more than 2.5 km and less than 3 km.

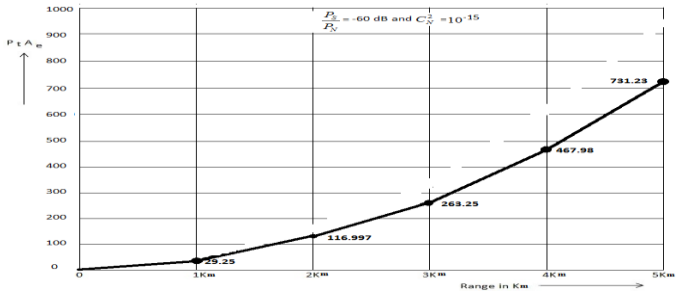

Fig 16. Power Aperture product versus Range for C_n^2= 10^{-15} and SNR = -60dB For our radar's 141.4 watt m^2 (P_t. A_e), range covered is up to 2.5 km for the above case. For 100 ns Baud time also the range covered is less than 1km.

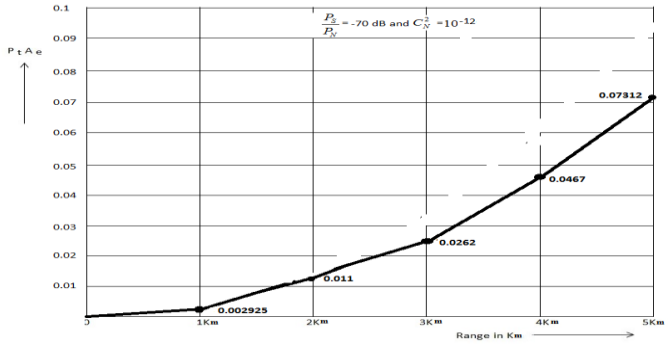

Fig 17. Power Aperture product versus Range for C_n^2= 10^{-12} and SNR = -70dB. For our radar's 141.4 watt m^2 (P_t. A_e), range covered is above 5km for the above case. For 100 ns Baud time also the range covered is more than 5 km. (P_t. A_e at 5 km =0.07312*6.25 =0.457).

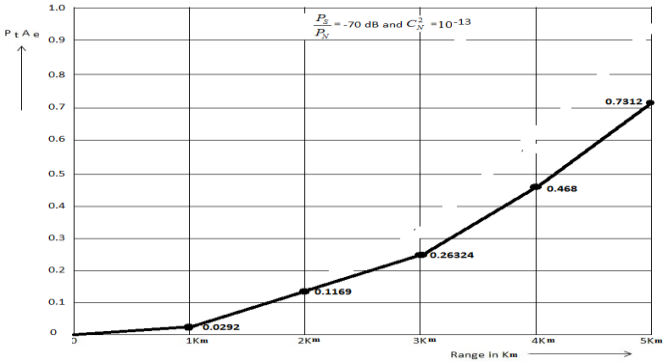

Fig 18. Power Aperture product versus Range for C_n^2= 10^{-13} and SNR = -70dB. For our radar's 141.4 watt m^2 (P_t. A_e), the range covered is above 5km for the above case. For 100 ns Baud time also the range covered is more than 5 km. (P_t. A_e at 5 km =0.7312*6.25 =4.57).

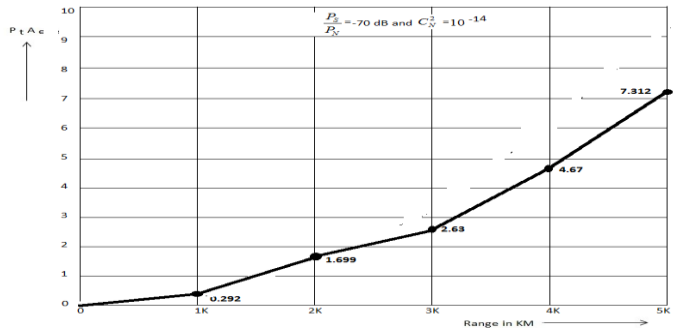

Fig 19. Power Aperture product versus Range for C_n^2= 10^{-14} and SNR = -70dB. For our radar's 141.4 watt m^2 (P_t. A_e), range covered is above 5 km for the above case. For 100 ns Baud time also the range covered is more than 5 km. (P_t. A_e at 5 km =7.312*6.25 =45.7).

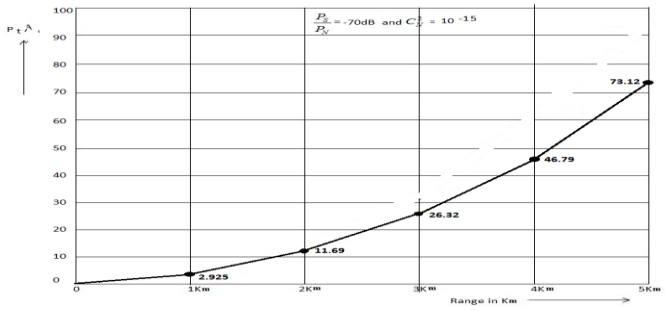

Fig 20. Power Aperture product versus Range for $C_n^2 = 10^{-15}$ and SNR = -70dB. For our radar's 141.4 watt m^2 (P_t. A_e), range covered is above 5 km for the above case. For 100 ns Baud time also the range covered is more than 2.5 km and less than 3 km.

- In clear Air conditions, received signals will be very weak in the absence of clouds and precipitation.
- In this mode there are two possible scattering mechanisms.
- 1. Scattering from refractive index gradients on scale of $\frac{\lambda}{2}$. This is often referred to as "Bragg scattering".

η = Reflectivity is proportional to $\lambda^{\frac{-1}{3}}$ in case of Bragg Scattering.

- 2. Particulate scattering from insects and birds.

b). Cloudy condition with precipitation

- Radar equation for distributed target like clouds or precipitation is given below.
- In this case, the beam is filled with targets as shown in the figure given below. $\Delta R = \frac{C\tau}{2}$

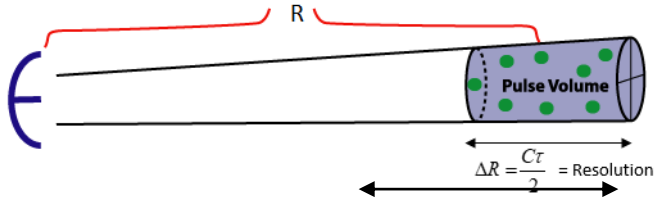

= Resolution

Fig 21. Radar equation for distributed target like clouds or p n below.

- In this case total average power is equal to the sum of powers scattered by individual scatters. Equation for average received power

$$P_S = \frac{P_t G_t G_r \delta\theta^2 \pi^3 \frac{C\tau}{2} |K|^2}{1024 Log_e^2 R^2 \lambda^2} \sum_i D_{ti}^6$$

also equal to

$$P_S = \frac{1}{2Log_e^2} \frac{P_t G_t G_r \lambda^2 \delta\theta^2 \pi^3 \frac{C\tau}{2} \eta}{512 \pi^2 R^2}$$

where $\eta = \sum_i \sigma_i$ = radar reflectivity = sum of all back scattering cross sections per unit volume. Back scattering cross section σ can be written as $\sigma = \frac{\pi^5 |K|^2 D_{ti}^6}{\lambda^4}$ Where D_{ti} = diameter of i^{th} target, λ = wave length, K = complex dielectric factor, it indicates how good a material is at back scattering radiation, For water $|K|^2$ =0.93, For ice $|K|^2$ =0.197, P_t = transmitted power, G_t = Transmitting antenna gain, G_r = Receiving antenna Gain, $\delta\theta$ = Beam width of antenna, τ = Baud time (sub pulse width), R =range and Finally Received power is equal to

$$P_S = \frac{P_t G_t G_r \delta\theta^2 \pi^3 \frac{C\tau}{2} |K|^2}{1024 Log_e^2 R^2 \lambda^2} \sum_i D_{ti}^6$$

[After substituting for σ]The following Signal and Noise power computations are made for Baud time of 250 ns. For 100 ns Baud time Noise power goes up by a factor of 2.5 and Signal power comes down by factor of 2.5 and Net Loss factor in SNR is equal to 6.25 (8dB).

Let us consider a case of single 1mm diameter water droplet in a volume of 1 m^3. In this case the average power received from a range of R= 3000 m and τ = 250 nS. P_t =20 Watts, G_t = 29.2 dB / 848.25 = gain of the transmitting antenna, G_r = 29.2 dB / 848.25 = gain of the receiving antenna, $\delta\theta$ = 5.7°= Beam width of antenna= 1/10th radian. λ = wave length $= \frac{3\times10^8}{1.4\times10^9} = 0.2143m$ R = Range = 3000 m, τ = Baud time (sub pulse width) = 250 ns, $|K|^2$ = for water = 0.93, $\sum_i D_{ti}^{\,6}$ = for 1mm diameter droplet of water = $D_{ti}^{\,6} = 10^{-18}$

$L_n2 = \text{Log}_e 2 = 0.69315$

$$P_S = \frac{20\times(848.25)^2\times\left(\frac{1}{10}\right)^2\times(3.142)^3\times37.5\times0.93\times10^{-18}}{1024\times0.69315\times(3000)^2\times(0.2143)^2} \quad P_S = \frac{155671994.9\times10^{-18}}{293368875.2}$$

$$= 5.30635X10^{-19}$$

P_N = noise power = 4x10 $^{-14}$ watts [already computed earlier]

SNR will be = $\frac{5.30635\times10^{-19}}{4\times\ 10^{-14}} = 1.3265\times10^{-5}$. With processing gain of 50dB, SNR will be equal to 1.3265. (in case of 100 ns Baud time, SNR = 0.212)

- If there are 10 droplets in 1 m^3 volume another 10dB improvement will be there in SNR. Then SNR will be 13.265. (In case of 100 ns Baud time, SNR = 2.12).
- Averaging for one second with a Radar PRF of 4000 and 1024 Baud code 66 dB (30dB due to 1024 Baud Code and 36 dB due to averaging data of 4000 transmitter pulses) processing Gain in SNR can be obtained.
- Total improvement will be (10dB + 66dB) = 76dB, in case 10 droplets are there in 1 m^3 volume. In this case SNR will be 530.6 (in case of 100 ns Baud time, SNR = 84.89).
- Averaging will be done as permitted by Doppler shift. In case of averaging for 100 pulses with 1024 bit code, SNR will be 53.06 (in case of 100 ns Baud time, SNR = 8.489). In case we make use of 32 bit code (Duty ratio of 3%) and average for 100 pulses, SNR will be 1.65. In case of 100 ns Baud time, SNR =0.264. Hence we have to average for more than 500 pulses to get SNR more than 1.

As per P_t. A_e(Power Aperture Product) graphs, we get signals up to 5 km range for a reflectivity factor of 10^{-14} for a peak power of 20 Watts and 3m diameter dish Antenna. For the reflectivity factors of 10^{-12} and 10^{-13}, we are much more comfortable with the received signals. These signal computations are applicable for clear air atmosphere. For precipitation studies, we get much better signals.

5.1 Improvement of Range Accuracy: The basic resolution provided by the sub pulse width of pseudorandom code of 250nS is 37.5m. For 100 ns Baud time the resolution is 15 m. The range accuracy of discrete targets can be improved further by using sliding correlates [using vernier principle] in which the receiver has got dual correlators one working at transmitter clock frequency and another one working at a slightly different frequency to get the required range accuracy improvement factor. However range accuracy improvement is limited by the Signal to Noise Ratio given by the formula $\Delta R = C\,\Delta t = \pm C\,\frac{Sub\ Pulse Width}{2\sqrt{\frac{S}{N}}}$, Example if $\frac{S}{N}$ =10 dB,

$$\Delta R \cong \pm C\,\frac{Sub\ Pulse Width}{2\times\sqrt{10}}$$

$$\cong \pm C\,\frac{Sub\ Pulse Width}{2\times3.16} \cong C\,\frac{Sub\ Pulse Width}{6}$$

Thus an improvement factor of 6 can be obtained. The first correlator works at a clock frequency of 4.0 MHz corresponding to 250 nS Baud time. The second one works at a clock frequency of 4.4MHz. In case of 100 ns Baud time, the clock frequencies are 10 MHz and 11 MHz

7.0 Experiment Results:

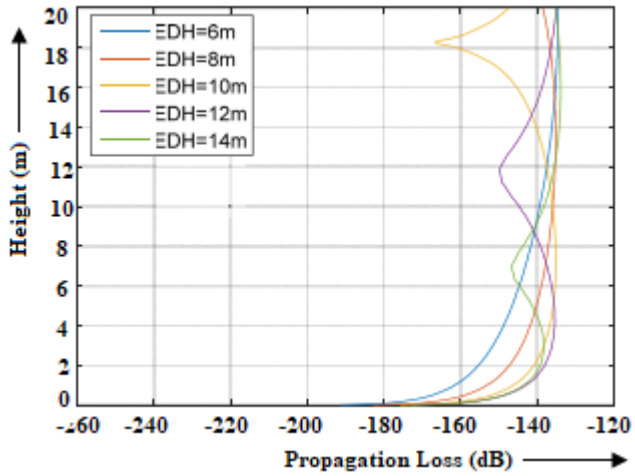

Fig 22. The figure shows the duct variation is drawn for different values of EDH is 6m, 8m, 10m, 12m and 14m. Above plots are drawn duct graphs with respect to height versus propagation loss.

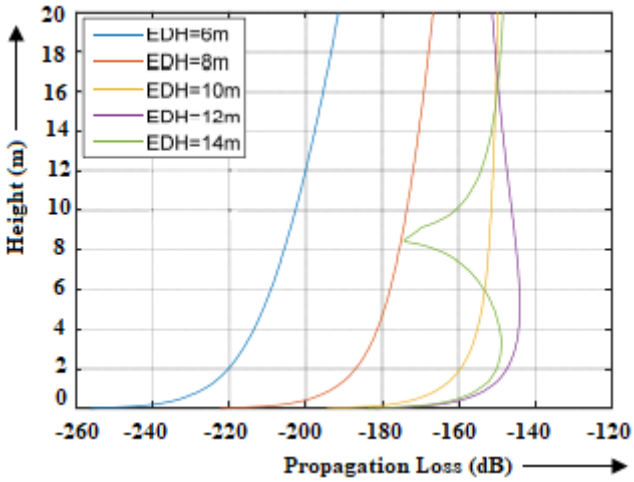

Fig 23 the figure shows the duct variation is drawn for different values of EDH is 6m, 8m, 10m, 12m and 14m. Above plots are drawn duct graphs with respect to height versus propagation loss with different timings.

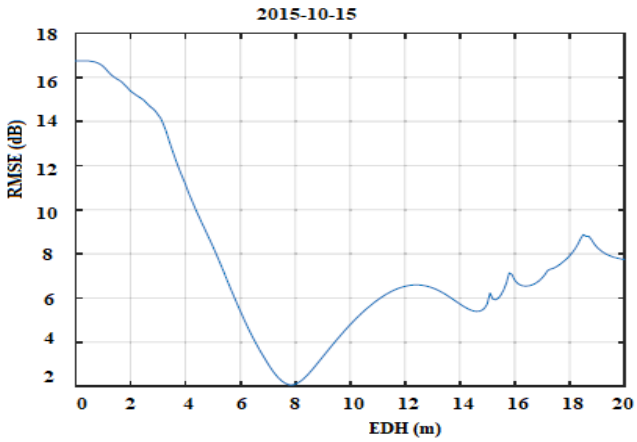

Fig. 23 shows root mean square error versus EDH and shows the 2 dBs RMSE error with height of 6 to 8meters.

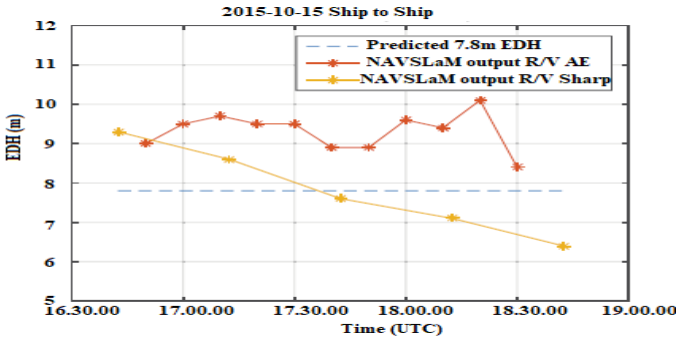

Fig. 24 shows the time versus EDH of propagation of rays from ship to ship communications during fourteenth October 2015.

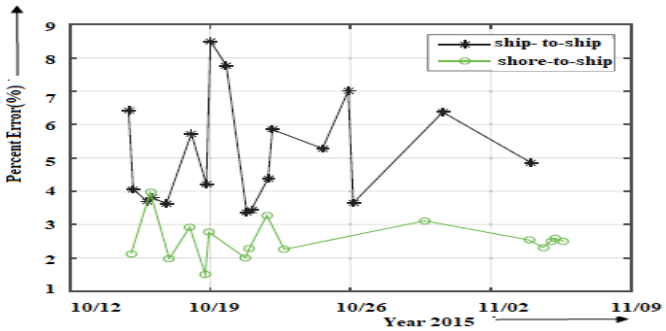

Fig. 25 shows rays are transmitted from ship to ship and ship to shore communications and plots are drawn between year and percentage of error present.

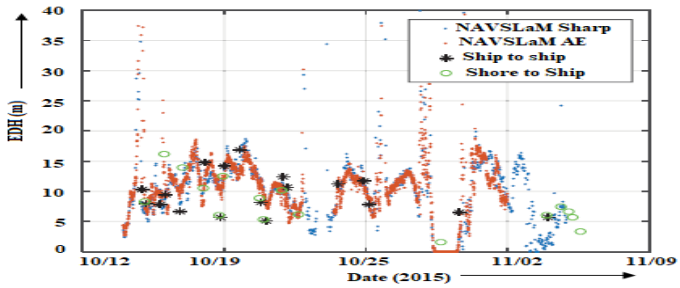

Fig. 26 shows the EDH at different heights with respect to year of data collected and variations of refractive index from ship to ship and ship to shore communications of electromagnetic wave representation.

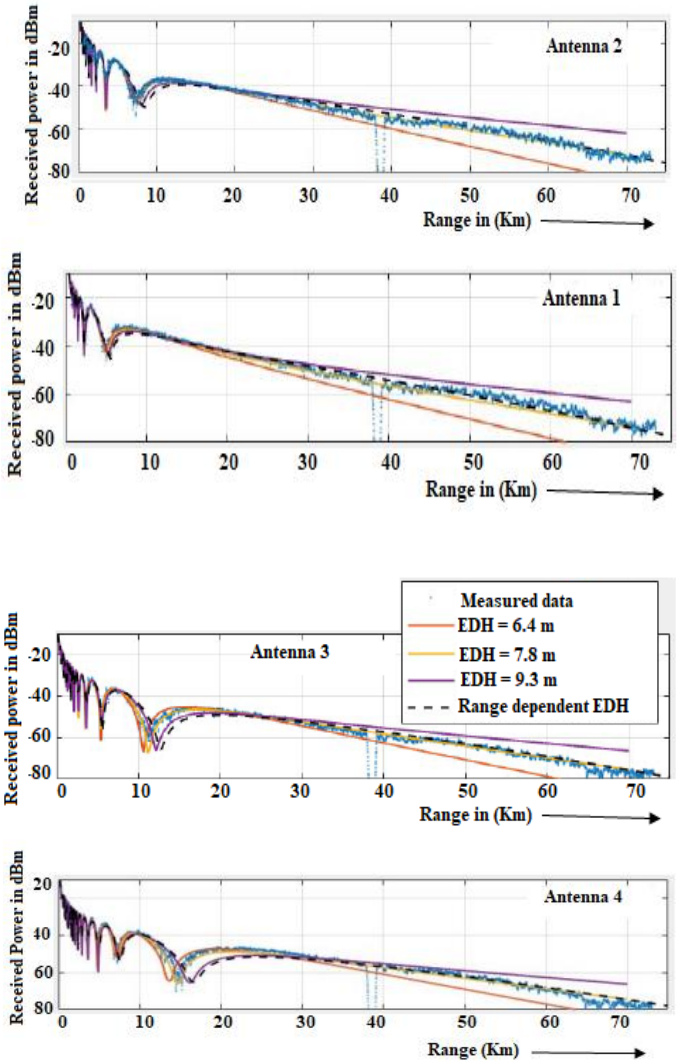

Fig. 27. Power received in dB from different antennas with different heights from free space on October month with two different weather conditions one is fixed EDH and other one is duct variation with different heights and transmitted signal frequency is 11.25GHz.

8. CONCLUSION

This paper clearly gives the information about x band frequency is used for transmission and array of signals are received from free space and analyzed from that Duct variation from season to season and time to time variation which is called Marine Duct environment. Four different antennas are placed at different places and with different heights and observed the received signals from that we can conclude that how the Duct environment in free space we can observe variations with existing ducting environment. Evaporation duct height is precisely estimated with long range of height and lower range of height from the earth's atmosphere out of which EDH values are predicted correctly for single range.

In this paper, for our designed radar of 141.4 watt m^2 (P_t. A_e) and 100 ns Baud Time we obtain the following distance with respect to C_n^2 and SNR.

Case -1	$C_n^2 = 10^{-13}$	SNR = -50dB	beyond 5 km	100 ns Baud time	up to 2.5 km.
Case -2	$C_n^2 = 10^{-14}$	SNR = -50dB	Up to 2.5 km.	100 ns Baud time	up to 1 km
Case -3	$C_n^2 = 10^{-15}$	SNR = -50dB	unto 500 meters	"	500 meters
Case -4	$C_n^2 = 10^{-12}$	SNR = -60dB	➢ 5km	"	➢ 5km
Case -5	$C_n^2 = 10^{-13}$	SNR = -60dB	➢ 5km	"	➢ 5km
Case -6	$C_n^2 = 10^{-14}$	SNR = -60dB	➢ 5km	"	➢ 2.5km
Case -7	$C_n^2 = 10^{-15}$	SNR = -60dB	Up to 2.5 km.	"	< 1 km
Case -8	$C_n^2 = 10^{-12}$	SNR = -70dB	➢ 5km	"	➢ 5km
Case -9	$C_n^2 = 10^{-13}$	SNR = -70dB	➢ 5km	"	➢ 5km
Case -10	$C_n^2 = 10^{-14}$	SNR = -70dB	➢ 5km	"	➢ 5km
Case -11	$C_n^2 = 10^{-15}$	SNR = -70dB	➢ 5km	"	Up to 2.5 km

And also observed the time versus EDH of propagation of rays from ship to ship communications during the fourteenth of October 2015. And when the rays are transmitted from ship to ship and ship to shore communications and plots are drawn between year and percentage of error present. And also EDH at different height to the year of data collected and variations of refractive index from ship to ship and ship to shore communications of electromagnetic wave representation. And also Power received in dB from different antennas with different heights from free space on October month with two different weather conditions one is fixed EDH and another one is duct variation with different heights and transmitted signal frequency is 11.25GHz.

REFERENCES:

[1] "Pulsed Doppler Digital Receiver for 2.5 MHz Partial Reflection Radar" presented at International Radar Symposium, India 2001, Bangalore 11-14 December 2001. This paper has been published in the proceedings of the symposium..

[2]."Doppler extraction from SODAR using complex covariance technique" presented at International Radar Symposium, India 2001, Bangalore 11-14 December 2001. This paper has been published in the proceedings of the symposium

[3]. "Partial Refle\ction Radar for the measurement of Mesispheric and Lower Thermospheric Drifts" – International Radar Symposium India 2003, Bangalore 2-5 December 2003. This paper has been published in the proceedings of the symposium.

[4]. "HF Backscatter Radar at the magnetic equator: System details and preliminary results". Published in the Indian Journal of Radio and Space Physics (IJRSP) Vol 30, April 2001 pp 77-90.

[5]. Satyanarayana M, Veerabuthiran S, Ramakrishna Rao D, Presennakumar B, Mohankumar S V, Muraleedharan Nair, S and Sreeja R, "Studies on tropospheric aerosol layers at a tropical coastal station, Trivandrum (8°33′ N, 77°E), India using lidar", National Space Science Symposium 2004, Kottayam, February 17-20, 2004.

[6]. Veerabuthiran S, Satyanarayana M, Ramakrishna Rao D, Presennakumar B, Mohankumar S V, Muraleedharan Nair, S and Sreeja R, "Lidar observations of cirrus clouds at low latitude tropical station, Trivandrum (8°33′ N, 77°E): General characteristics", National Space Science Symposium 2004, Kottayam, February 17-20, 2004.

[7]. Satyanarayana M, Ramakrishna Rao D, Muralidharan Nair, S, Mohankumar S V, Presennakumar B, Veerabuthiran S, and Sreeja R, "High Resolution Imaging Laser Altimeter for Interplanetary Missions", National Space Science Symposium 2004, Kottayam, February 17-20, 2004.

[8]. Veerabuthiran S, Satyanarayana M, Ramakrishna Rao D, Presennakumar B, Mohankumar S V, Muraleedharan Nair, S and Sreeja R, "Temperature dependences of stratospheric aerosol extinction observed at a low latitude station, Trivandrum (8°33′ N, 77°E), India using lidar", SPARC 2004.

[9]. Veerabuthiran S, Satyanarayana M, Ramakrishna Rao D, Presennakumar B, Mohankumar S V, Muraleedharan Nair, S and Sreeja R, "Cirrus clouds observed near the low latitude tropical tropopause using ground based lidar", SPIE-Remote Sensing 2004

[10].Satyanarayana M, Veerabuthiran S, Ramakrishna Rao D, Presennakumar B, Mohankumar S V, Muraleedharan Nair, S and Sreeja R, "Winter monsoon variation of lower tropospheric aerosol layers at a tropical coastal station, Trivandrum (8°33′ N, 77°E), India", COSPAR 2004.

[11].P. A. Frederickson, "Further improvements and validation for the navy atmospheric vertical surface layer model (navslam)," in *Proc USNCURSI Radio Sci. Meeting (Joint AP-S Symp.)*, Jul. 2015, p. 242.

[12]. Veerabuthiran, S., Satyanarayana, M., Ramakrishna ao, D., Presennakumar, B. and Mohankumar, S. V. "Lidar studies on the seasonal variations of tropospheric aerosol structure and cirrus clouds at a tropical station, Trivandrum (8°33′N, 77°E), India" submitted to SPIE-meeting, Washington (USA), July 7-12, 2002.

[13].Satyanarayana, M., Ramakrishna Rao, D., Presennakumar, B. Mohankumar, S. V. and Veerabuthiran, S. "Influence of atmospheric conditions on the performance of IR volume imaging lidar system" submitted to SPIE-meeting, Washington (USA), July 7-12, 2002.

[14]. Satyanarayana, M., Veerabuthiran, S., Ramakrishna Rao, D., Presennakumar, B., and Mohankumar S V.," Multiwavelength lidar studies of aerosol, cirrus clouds and temperature of the atmosphere: Results from a low latitude coastal station, Trivandrum, India" NCST 2002, September 28-29, New Delhi.

[15]. Satyanarayana, M., Veerabuthiran, S., Ramakrishna Rao, D., Presennakumar, B. and Sreelatha, P. "Multiwavelength lidar studies on aerosol extinction and temperature structure at Trivandrum" COSPAR-2000, Warsha, July 16-23.

[16]. Satyanarayana, M., Veerabuthiran, S., Ramakrishna Rao, D., Presennakumar, B. and Sreelatha, P. "Preliminary studies with multiwavelength lidar on aerosol extinction and temperature structure at Trivandrum", NSSS-2K, Puri, March 1-4.

[17].Satyanarayana, M., Ramakrishna Rao, D., Presennakumar, B., Mohankumar, S. V. and Veerabuthiran, S. "Multiwavelength laser radar studies in the atmosphere", INCOLA-2000, Tiruchirappalli, March 1-4, 2000.

[18]. "Retrieval of Optical Properties of Clouds and Aerosols from a Space Borne Lidar", Abstracts of International Conference on Optics and Optoelectronics (ICOL-2005), IRDE, Dehradun, India, December 12-15, 2005, pp 520.

[19]. "Role of Transport on the Lower Tropospheric Aersol Layers observed at a Trpical Coastal Station, Trivandrum (8°33'N, 77°E), India using Lidar", Proc. of the 4th Asian Aerosol Conference (AAC-2005), Mumbai, December 13-16, 2005, IASTA Bulletin, Vol. 17, December 2005, pp 467-468.

[20]. "Intricacies of data acquisition and processing systems of atmospheric radars and lidars".Authors: Prof. D. Ramakrishna Rao, P Sudhakar, P. Kalavathi, and Dr M. Satyanarayana, Conference: National Conference on Role of Radars in Atmospheric and ionospheric studies, KL University, Vijayawada, January, 2012.

[21] H. E. Bussey and G. Birnbaum, "Measurement of variations in atmospheric refractive index with an airborne microwave refractometer," *J. Res. Nat. Bur. Standards*, vol. 51, no. 4, pp. 171–178, 1953.

[22] J. R. Rowland and S. M. Babin, "Fine-scale measurements of microwave refractivity profiles with helicopter and low-cost rocket probes," *Johns Hopkins APL Tech. Dig*, vol. 8, no. 4, pp. 413–417, 1987

[23] A. R. Lowry, C. Rocken, S. V. Sokolovskiy, and K. D. Anderson,"Vertical profiling of atmospheric refractivity from ground-based GPS,"*Radio Sci.*, vol. 37, no. 3, pp. 13-1–13-19, 2002.

[24]. A. Willitsford and C. R. Philbrick, "Lidar description of the evaporative duct in ocean environments," *Proc. SPIE*, vol. 5885, Sep. 2005, Art. no. 58850G.

[25]. J. L. Krolik and J. Tabrikian, "Tropospheric refractivity estimation using radar clutter from the sea surface," in *Proc. 1997 Battlespace Atmospherics Conf., SPAWAR Syst. Command Tech. Rep.*, vol. 2989,pp. 635–642, Mar. 1998.

[26] L. T. Rogers, C. P. Hattan, and J. K. Stapleton, "Estimating evaporation duct heights from radar sea echo, *Radio Sci.*, vol. 35, no.4, pp. 955–966, 2000.

[27]. C. Yardim, P. Gerstoft, and W. S. Hodgkiss, "Estimation of radio refractivity from Radar clutter using Bayesian Monte Carlo analysis," *IEEE Trans. Antennas Propag.*, vol. 54, no. 4, pp. 1318–1327, Apr. 2006.

[28].A. E. Barrios, "Estimation of surface-based duct parameters from surface clutter using a ray trace approach," *Radio Sci.*, vol. 39, no. 6, RS6013, pp. 1–15, 2004.

[29].R. M. Hodur and J. D. Doyle, "The coupled ocean/atmosphere mesoscale prediction system (COAMPS)," *Coastal Ocean Prediction*, vol. 56,pp. 125–156, 1999.

[30]. A. S. Monin and A. M. F. Obukhov, "Basic laws of turbulent mixing in the surface layer of the atmosphere," *Contrib. Geophys. Inst. Acad. Sci.USSR*, vol. 151, pp. 163–187, Sep. 1954.

[31]. "Design and Development of compact aerosols and cloud lidar and simulations on the possible scientific studies". Authors: Prof. D. Ramakrishna Rao, P Sudhakar, P. Kalavathi, and Dr M. Satyanarayana,Conference: National Space Science Symposium, SV University, Tirupati,February, 2012.

[32]."Siganal Procesing for Atmospheric Wind Profiling Radars"Authors: P. Kalavathi, Prof. D. Ramakrishna Rao, P Sudhakar, and Dr M. SatyanarayanaConference: National Conference on Emerging trends in Siganl Processing ana Embedded Systems, Geethanjali College,Cheeryal(V), Keesara(M), R.R DIST

[33].Inversion Solutions for Lidar Back scattered signal.Authors:P. Sudhakar, P. Kalavathi D. Ramakrishna Rao, and M. Satyanarayana. Conference: International Conference on Innovations in Electronics and Communication Engineering (ICIECE-2012) July 20-21,

[34]"Design and Development of a Satellite based Lidar System in the Indian context", Abstracts of International Conference on Optics and Optoelectronics (ICOL-2005), IRDE, Dehradun, India, December 12-15, 2005, pp 521.

.